CrystEngComm

PAPER

View Article Online
View Journal | View Issue

Cite this: *CrystEngComm*, 2024, **26**, 4431

Extended viologen compounds with photochromism, photoresponsive luminescence and ultrahigh quenching efficiency†

Lu Liu,[a] Le-Tian Zhang,[a] Feng-Chen Yuan,[a] Hong-Xia Ren,*[a] Yue Ma [a] and Qing-Lun Wang *[b]

Received 20th June 2024,
Accepted 26th July 2024

DOI: 10.1039/d4ce00615a

rsc.li/crystengcomm

A new type of extended viologen, *N*,*N*′-2,5-bis(3-pyridinium)thiazolo[5,4-*d*]thiazole dipropionate, (m-H_2-TTzPA)$(HSO_3)_2$ (**1**), was synthesized, and two new coordination polymers, $\{[Cd(m\text{-}TTzPA)Br_2]\cdot H_2O\}_n$ (**2**) and $\{[Zn(m\text{-}TTzPA)Br_2]\cdot H_2O\}_n$ (**3**), were prepared based on the m-TTzPA ligand. Compounds **1–3** exhibit photochromic behaviors, which were proved using single-crystal X-ray diffraction, UV-vis spectroscopy and EPR characterizations. Furthermore, all the compounds have obvious fluorescence quenching behaviors upon irradiation using a xenon lamp, where compound **1** exhibits a significant quenching efficiency of 95.84%.

Introduction

Photochromism is a reversible photoinduced transformation of a molecule between two isomers whose absorption spectra are distinguishably different.[1–3] In general, photogenerated colored isomers can return to the original forms either photochemically or thermally. These materials have clever structural design and potential application in molecular switching, nondestructive readout, photomagnetism, inkless and erasable printing and optical memory devices.[4–16] As we know, 1,1′-disubstituted 4,4′-bipyridinium derivatives (viologens) are known as a class of organic functional ligands for the construction of photochromic materials and have been widely used in molecular assembly owing to their photo-induced electron transfer (PET) process.[17,18] Recently, a class of so-called "extended viologens" have come into the view of scientists because of their strongly conjugated system consisting of two pyridinium rings spaced by conjugating groups, such as thiazolothiazole.[19] For example, Py_2TTz (2,5-bis(4-pyridinyl)thiazolo[5,4-*d*]thiazole), a typical extended viologen, has similar PET properties to viologen derivatives but also has unique luminescent properties. Walter's research group composited a suite of extended viologen compounds, *N*,*N*′-dialkyl and *N*,*N*′-dibenzyl-2,5-bis(4-pyridinium)thiazolo[5,4-*d*]thiazole derivatives,[20] demonstrating high fluorescent quantum efficiency and reversible electrochromic behavior. Besides, Gao *et al.* modified Py_2TTz with a carboxylate group to obtain a novel viologen ligand TTVTC (2,5-bis(pyridinium-4-yl)thiazolo[5,4-*d*]thiazole tetracarboxylate) and a novel photochromic Cd-based MOF.[21] Our group also synthesized two new Zn-related compounds and investigated their photochromic behavior using the viologen ligand of TTVP (2,5-bis(pyridinium-4-yl)thiazolo[5,4-*d*]thiazole propionate).[22]

Herein, we synthesized a new type of extended viologen of *N*,*N*′-2,5-bis(3-pyridinium)thiazolo[5,4-*d*]thiazole dipropionic acid hydrogen sulfite, ((m-H_2TTzPA)$(HSO_3)_2$, **1**) and used it as a ligand to construct two novel photochromic coordination polymers, $\{[Cd(m\text{-}TTzPA)Br_2]\cdot H_2O\}_n$ (**2**) and $\{[Zn(m\text{-}TTzPA)Br_2]\cdot H_2O\}_n$ (**3**). The photoinduced electron transfer from donors to acceptors not only influences absorption bands, but also influences the transition of fluorescence emission. Therefore, all the compounds can present colour changes and photoresponsive luminescence behaviours. Moreover, the significant value of 95.84% for **1** is the highest quenching efficiency as far as we know.

Experimental

Materials and methods

All reagents were purchased commercially and used without further purification. C, H, N elemental analysis was performed on an Elementar Vario EL Cube analyzer. A powder X-ray diffraction (PXRD) pattern was collected at room temperature using a Rigaku D/max-2500 diffractometer with Mo-Kα radiation (λ = 0.71073 Å). At room temperature, a UV-visible absorption spectrum was recorded in the reflection

[a] *College of Chemistry, Nankai University, Tianjin, 300071, P. R. China. E-mail: csxh3605@sina.com.cn*
[b] *Key Laboratory of Advanced Energy Materials Chemistry (Ministry of Education), Nankai University, Tianjin, 300071, P. R. China. E-mail: wangql@nankai.edu.cn*

† Electronic supplementary information (ESI) available: Tables S1–S3, Fig. S1 and S2. X-ray crystallographic files for **1–3**: CCDC 2356753–2356755. See DOI: https://doi.org/10.1039/d4ce00615a

mode on a Persee TU1901 UV-visible spectrophotometer with an integrating sphere attachment and 0.8 g $BaSO_4$ particles as the background. Granules to be tested were made of a mixture of 0.65 g $BaSO_4$ and 0.15 g samples. Infrared spectra were recorded on a Bruker Alpha FT-IR spectrophotometer in the 4000–400 cm^{-1} area. Electron paramagnetic resonance (EPR) spectra were recorded on a Bruker EMX-6/1 spectrometer at 9.844 GHz magnetic field in the X-band at room temperature. Fluorescence spectra were measured with an FL-4600 fluorescence spectrometer (Hitachi, Japan). A 300 W xenon lamp (PLS-SXE 300C) system equipped with an infrared filter was used to illuminate the samples to obtain various spectra. The distance between these samples and the Xe lamp was 30 cm (Scheme 1).

Synthesis of 2,5-di (pyridin-3-yl)thiazolo[5,4-*d*]thiazole m-TTz. m-TTz was synthesized according to the similar literature procedures of 2,5-di (pyridin-4-yl)thiazolo[5,4-*d*] thiazole using 3-pyridinecarboxaldehyde instead of 4-pyridinecarboxaldehyde.[23]

Synthesis of *N*,*N*′-2,5-bis(3-pyridinium)thiazolo[5,4-*d*] thiazole dipropionic acid hydrogen sulfite, (m-H_2TTzPA)$(HSO_3)_2$ (1). m-TTz (8.1 mmol, 2.4 g) and acrylic acid (30 mL) were added to a 250 mL round bottomed flask, followed by 150 mL ethanol. The mixture was refluxed for 10 h and then cooled to room temperature. The resulting precipitate was filtered to get the green crude product, which was dissolved in 50 mL methanol and then recrystallized by adding ethyl acetate. Yield 42%. Anal. calcd (%) for $C_{10}H_{10}N_2O_5S_2$: C 39.72, H 3.33, N 9.27; found: C 39.54, H 3.15, N 9.13.

Synthesis of $\{[Cd(m\text{-}TTzPA)Br_2]\cdot H_2O\}_n$ (2). (m-H_2TTzPA)$(HSO_3)_2$ (0.3 mmol, 0.0907 g) was dissolved in 10 mL H_2O and $CdBr_2$ (0.3 mmol, 0.0817 g) was dissolved in 5 mL H_2O. Both solutions were mixed and stirred at 95 °C for 20 min and then cooled to room temperature. 5 mL EtOH was then added to the mixed solution. Green flaky crystals were obtained after evaporation at room temperature for 3 days. Yield: 28% (based on Cd). Anal. calcd (%) for $C_{20}H_{18}Br_2CdN_4O_5S_2$: C 32.87, H 2.48, N 7.67; found: C 32.94, H 2.35, N 7.58.

Synthesis of $\{[Zn(m\text{-}TTzPA)Br_2]\cdot H_2O\}_n$ (3). Complexes **3** were synthesized by the same method as **2** using $ZnBr_2$ (0.3 mmol, 0.0675 g) instead of $CdBr_2$. Yield 32% (based on Zn). Anal. calcd for $C_{20}H_{18}Br_2ZnN_4O_5S_2$: C 35.13, H 2.65, N 8.19; found: C 35.38, H 2.42, N 8.22.

X-ray diffraction analysis

The diffraction intensities for compounds **1–3** were collected on a computer-controlled Rigaku 007 Saturn 70 diffractometer using the ω-scan technique with graphite-monochromated Mo-K_α radiation (0.71073 Å) or Cu-K_α radiation (1.54184 Å). Also, lorentz polarization and absorption corrections were applied. Using the *SHELXS* program in the *SHELXTL* software package[24] or the *Olex2* software,[25] the structures were solved by direct methods and refined with the full-matrix least-squares technique. Anisotropic thermal parameters were assigned to all non-hydrogen atoms. Hydrogen atoms were placed in calculated positions and refined as riding atoms with a common fixed isotropic thermal parameter. Table 1 summarizes the detailed crystallographic data and structure refinement parameters of compounds **1–3**. Tables S1–S3† list the key lengths and angles for compounds **1–3**.

Results and discussion

Crystal structure

Single-crystal X-ray structure analysis revealed that compound **1** crystallized in the monoclinic $P2(1)/n$ space group. The asymmetric unit comprises half a protonated m-H_2TTzPA^{2+} cation and one hydrogen sulfite anion, as shown in Fig. 1a. m-H_2TTzPA^{2+} cations were then arranged in one dimensional through π···π interactions between pyridine and thiazole rings since the distance between the adjacent pyridine ring and thiazole ring is 3.4162 Å (Fig. 1b).

Compound **2** crystallized in the triclinic $P\bar{1}$ space group. The asymmetric unit is composed of one Cd(II) ion, two halves of m-TTzPA ligands, two bromide anions and one H_2O molecule, as shown in Fig. 2a. The Cd(II) center is five-

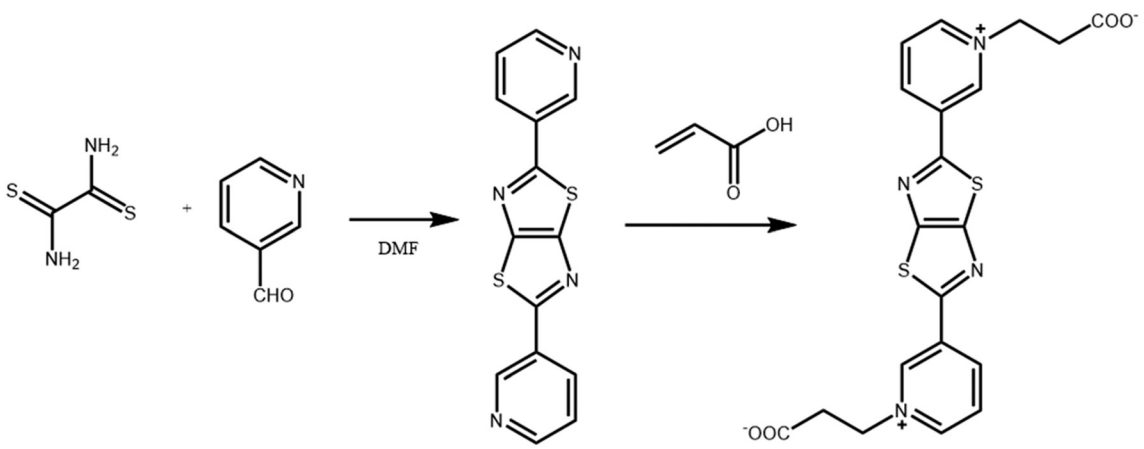

Scheme 1 The synthesis process for m-TTzPA.

Table 1 Crystallographic data and structural refinement for compounds 1–3

Compound	1	2	3
Empirical formula	$C_{10}H_{10}N_2O_5S_2$	$C_{20}H_{18}Br_2CdN_4O_5S_2$	$C_{10}H_9BrN_2O_{2.50}SZn_{0.50}$
Formula weight	302.32	730.73	341.85
Temperature	100(2) K	293(2) K	100(2) K
Crystal system	Monoclinic	Triclinic	Monoclinic
Space group	$P2(1)/n$	$P\bar{1}$	$C2/c$
a/Å	5.49590(10)	8.3132(2)	11.9566(4)
b/Å	15.2745(3)	8.5739(2)	12.1665(3)
c/Å	13.9065(2)	16.6728(4)	16.0453(5)
α/°	90	81.781(2)	90
β/°	90.7560(10)	88.042(2)	92.158(3)
γ/°	90	89.048(2)	90
V/Å^3	1167.31(4)	1175.40(5)	2332.45(12)
Z	4	2	8
D_{calc}/g cm^{-3}	1.720	2.059	1.947
μ/mm^{-1}	4.356	13.452	4.700
F(000)	624	708	1352
Radiation	CuKα (λ = 1.54184 Å)	CuKα (λ = 1.54184 Å)	MoKα (λ = 0.71073 Å)
θ range for data collection/°	4.30 to 76.27	5.21 to 75.89	2.39 to 29.40
Reflections collected	5731	11 327	7280
Independent reflections	2343 [R_{int} = 0.0319, R_{sigma} = 0.0335]	4701 [R_{int} = 0.0251, R_{sigma} = 0.0305]	2561 [R_{int} = 0.0215, R_{sigma} = 0.0267]
Data/restraints/parameters	2343/0/174	4701/0/307	2561/0/158
Goodness-of-fit on F^2	1.094	1.095	1.037
Final R indices [$I > 2\sigma(I)$]	R_1 = 0.0417, wR_2 = 0.1123	R_1 = 0.0299, wR_2 = 0.0795	R_1 = 0.0216, wR_2 = 0.0533
R indices (all data)	R_1 = 0.0439, wR_2 = 0.1136	R_1 = 0.0321, wR_2 = 0.0802	R_1 = 0.0261, wR_2 = 0.0545

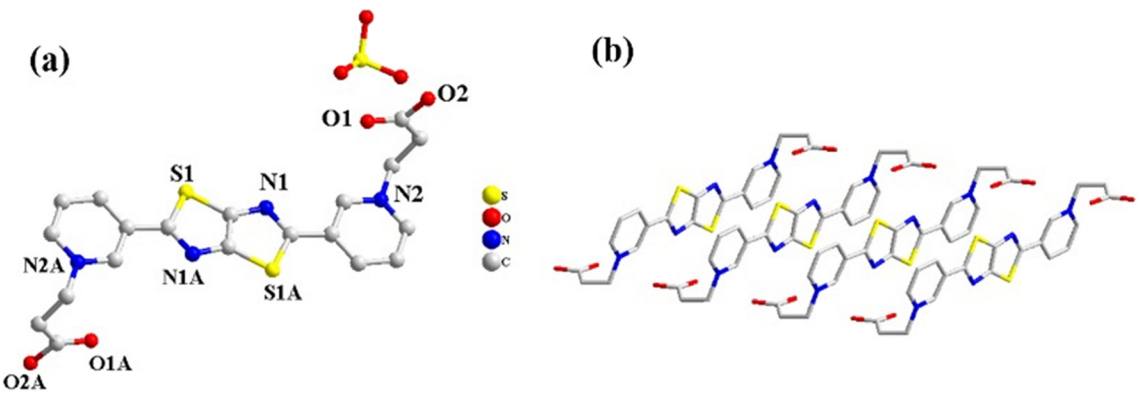

Fig. 1 (a) Crystal structure of compound 1, [A][−x, 1 − y, and 1 − z]; (b) π···π interactions between pyridine and thiazole rings.

coordinated by three oxygen atoms from two m-TTzPA ligands and two bromide anions. The Cd–O bond lengths are in the range of 2.186 Å to 2.404 Å, while the Cd–Br bond lengths are much longer (2.5731 Å to 2.5769 Å). There are two kinds of m-TTzPA ligands in compound 2, one is the unidentate coordination mode and the other one is the bidentate coordination mode. The adjacent Cd(II) ions are connected by two kinds of m-TTzPA ligands alternately to form a one-dimensional structure (Fig. 2b). π···π interactions can also be found between different chains since the distance between the coplanar m-TTzPA ligands is 3.6699 Å (Fig. 2c).

Compound 3 crystallized in the monoclinic $C2/c$ space group. The asymmetric unit is composed of half a Zn(II) ion, half a m-TTzPA ligand, one bromide anion and half a H_2O molecule. The Zn(II) center is four-coordinated by two oxygen atoms from two m-TTzPA ligands and two bromide anions (Fig. 3a). The Zn–O and Zn–Br bond lengths are 1.9663 Å and 2.3852 Å, respectively. The adjacent Zn(II) ions are also connected by m-TTzPA ligands by unidentate coordination mode to form a one-dimensional structure (Fig. 3b). π···π interactions can also be found between different chains since the distance between the coplanar m-TTzPA ligands is 3.562 Å.

Photochromic properties

Compounds 1–3 readily show photochromic behaviors at ambient conditions. Under Xe-lamp irradiation, the green powder sample of 1 turns brown after 10 s and reaches saturation after 20 min, while 2 and 3 turns from green to brown in 20 seconds and approaches the saturation after about 60 min. The photoproducts can return to their original color after being left in darkness for 1 days or heated at 95 °C for 2 h. UV-vis spectroscopy was used to detect the photochromic processes. The new broadband at *ca.* 545 nm

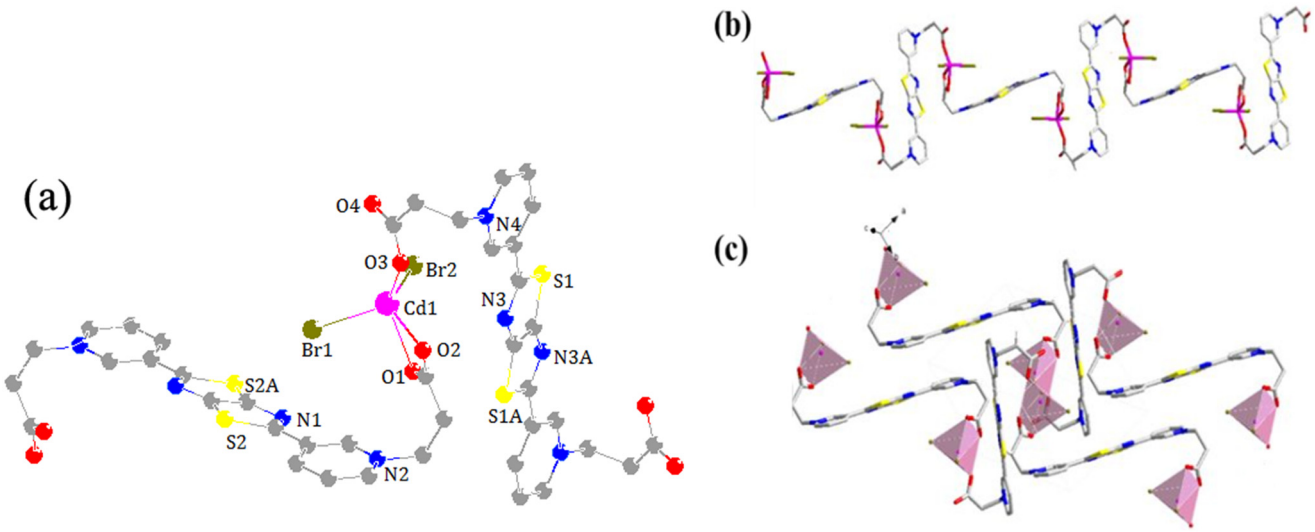

Fig. 2 (a) Coordination environments of the Cd(II) ion, (b) 1D structure of **2**, and (c) π···π interactions between different chains.

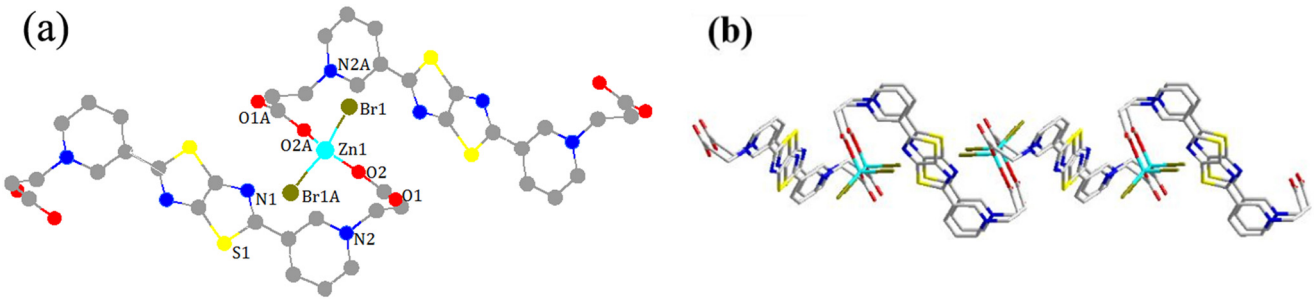

Fig. 3 (a) Coordination environments of the Zn(II) ion, ^{A}[1 − *x*, *y*, 1/2 − *z*], ^{B}[1 − *x*, *y*, 1/2 − *z*], and (b) 1D structure of **3**.

for **1** (570 nm for **2** and 551 nm for **3**) emerges after irradiation, and these absorption bands gradually rise upon increasing the exposure time (Fig. 4). However, the extent of increase for compounds **2** and **3** are much less than that of compound **1**. The above facts indicate that the photochromic behavior mainly results from the m-TTzPA ligand, while metal ions have little influence or even a negative effect on it.

Assuming that the photochromic behavior is based on the first-order kinetics, according to the Lambert–Beer law $\ln(A_0 - A)/(A_t - A) = kt$, where k is the reaction rate constant, A_0, A_t, and A represent absorbance at initial, t and saturation time, respectively, and the UV-vis data at 545.5 nm for **1** (569.5 nm for **2** and 551 nm for **3**) can be linearly fitted. Rate constants (k) are 3.13×10^{-3} s^{-1} (R^2 = 0.9884) for **1**, 6.28×10^{-4} s^{-1} (R^2 = 0.9725) for **2** and 9.34×10^{-4} s^{-1} (R^2 = 0.9806) for **3**, respectively (Fig. 4).[19] It is obvious that **1** has the most sensitive response upon radiation, and then **3**, while **2** is relative insensitive to ultraviolet light.

EPR measurements indicate that the original state of compounds **1–3** has a weak signal, which is most likely caused by daylight. Upon radiation, obvious radical signals with g = 2.00 emerge after the Xe-lamp stimulus (Fig. 5), which are close to the single-electron signal peak at g = 2.0023.[26] The results clearly suggest that the photochromic phenomena of **1–3** are attributed to the generation of radical species. Moreover, the PXRD patterns (Fig. S1†) and IR spectra (Fig. S2†) remain basically unchanged after irradiation, indicating that the photochromism of **1–3** is not relevant to light-induced isomerization or dissociation. This means that light stimulation results in photoinduced electron transfer (PET) and produces radical species, causing a color change.[21,22]

By analyzing the crystal structure, the closest distance between carboxylate O and pyridinium N is 3.0409 Å for **1** and the π···π distances are 3.4162 Å (Fig. 6), which are all suitable for electron transfer. By contrast, the distance between carboxylate O and pyridinium N are 3.2189 Å and 3.1109 Å in **2** while 3.0180 Å in **3**, and the π···π distances are 3.6699 Å and 3.562 Å for **2** and **3** (Fig. 6), respectively. In several examples of photochromic compounds, carboxylate groups can act as electron donors and pyridines accept electrons.[27–29] Using this principle, the carboxylate O of m-TTzPA donates electrons to pyridinium N under irradiation, and π···π stacking interactions may also serve to transfer electrons.[30] By the comprehensive analysis of both the distance between the carboxylate O and pyridinium N and π···π distances, compound **1** has the best electron transfer pathway, which may be the main reason why **1** has faster photoreaction rate than **2** and **3**.

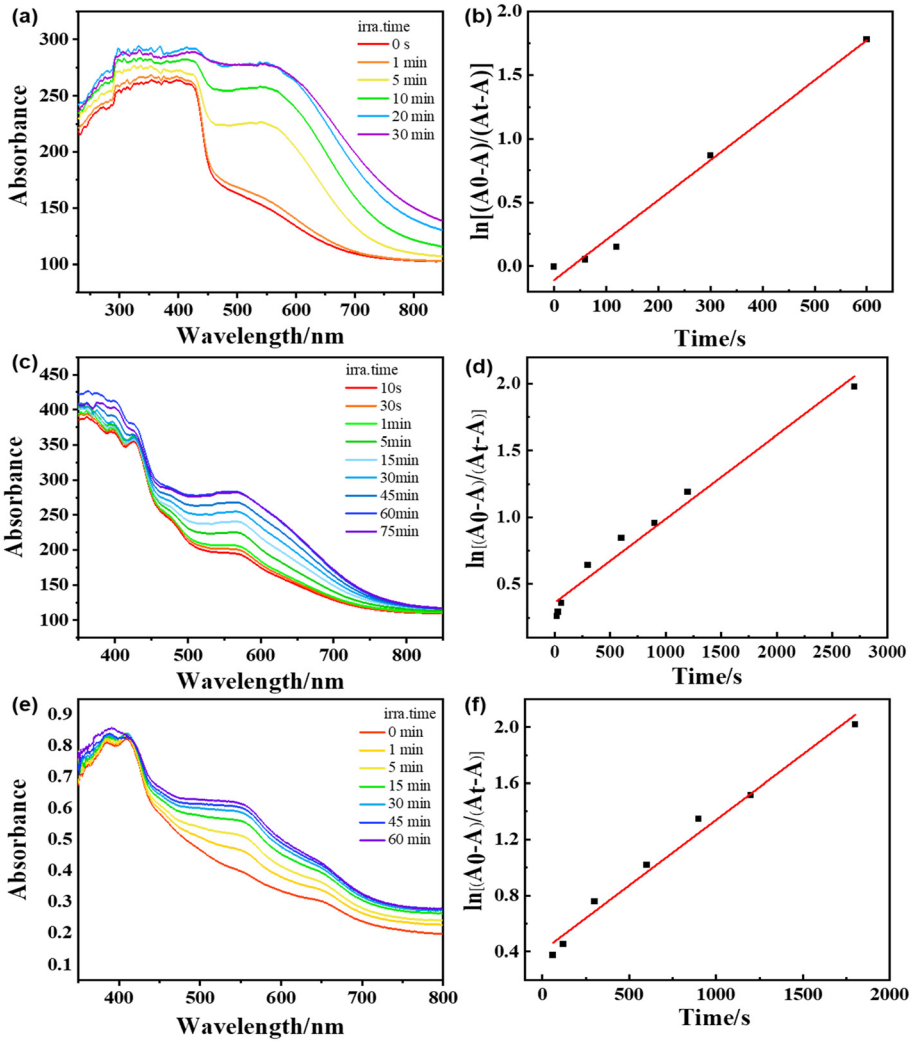

Fig. 4 Time-dependent UV-vis spectra of **1** (a), **2** (c), and **3** (e) upon irradiation and solid-state first-order rate plot under photoirradiation of **1** (b), **2** (d), and **3** (f).

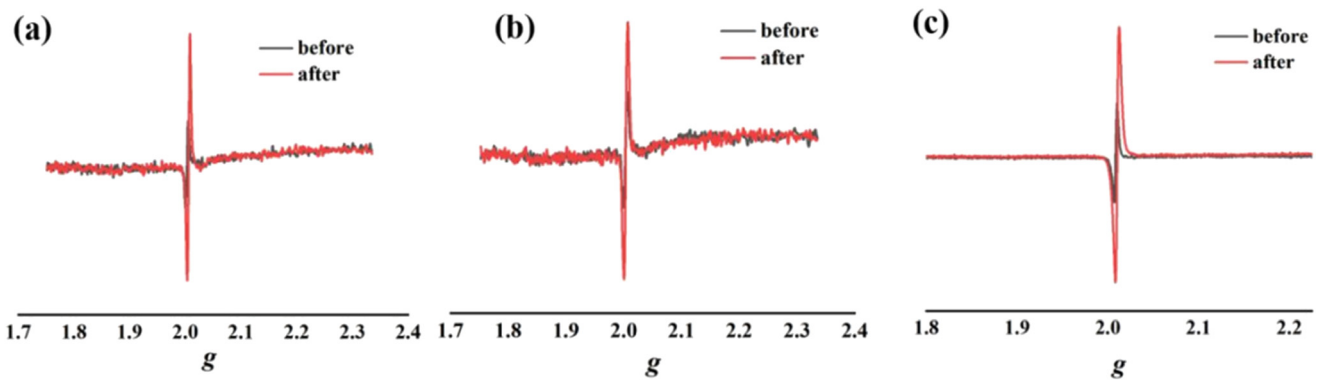

Fig. 5 ESR spectra of **1** (a), **2** (b) and **3** (c) before and after irradiation.

Luminescence properties

Photo-controlled luminescence properties are usually mentioned in the study of photochromic materials as another product of the electron transfer process.[31–33] The fluorescence properties of compounds **1–3** was investigated in the solid state at room temperature. As shown in Fig. 7, there is a strong emission peak at 464 nm upon excitation at 370 nm in compound **1**. Meanwhile, compound **2** shows strong emission peak at 463 nm upon excitation at 371 nm and strong emission

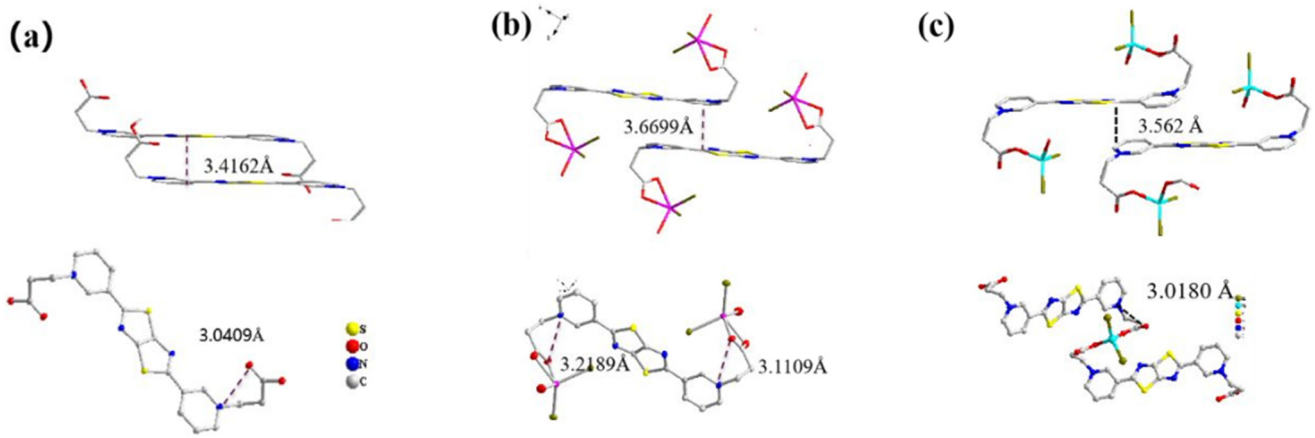

Fig. 6 Possible PET pathways in **1** (a), **2** (b) and **3** (c).

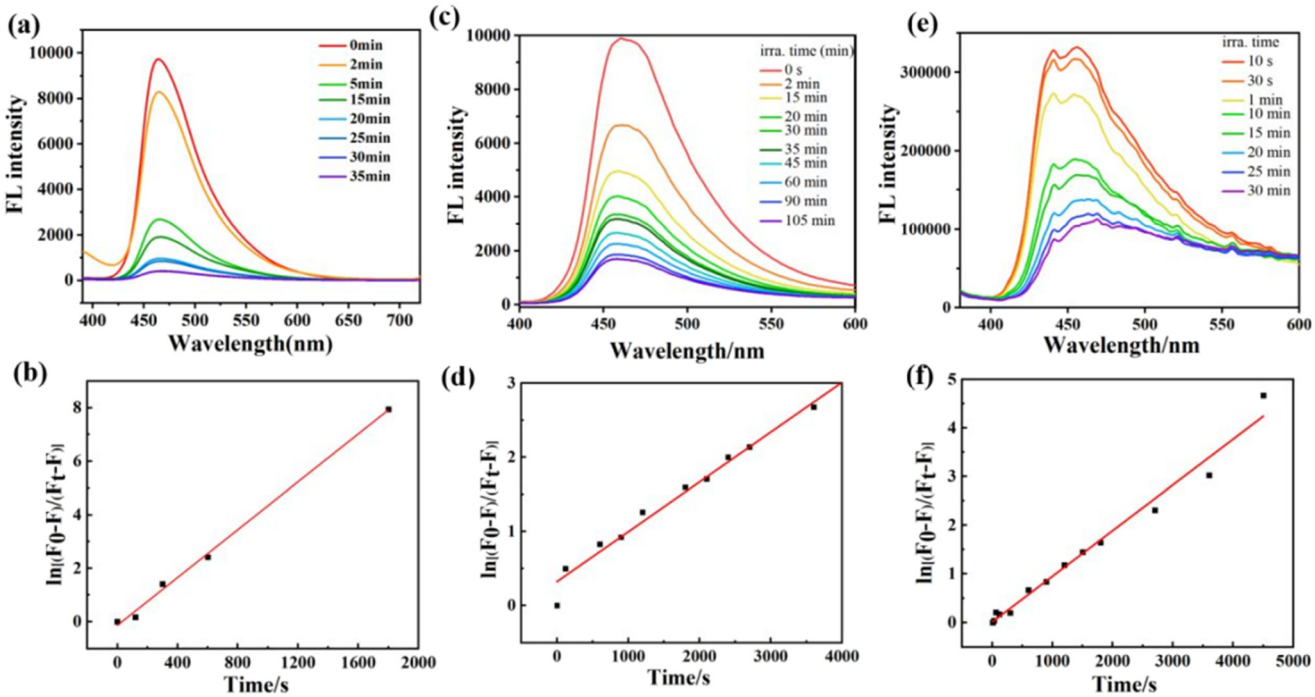

Fig. 7 Photo-controlled fluorescence spectra of **1** (a), **2** (c) and **3** (e) over irradiation time and solid-state first-order rate plot of the fluorescence spectra for **1** (b), **2** (d), and **3** (f).

peak at 466 nm upon excitation at 358 nm can be found in compound **3**. These emissions could be attributed to m-TTzPA itself and the effect of metal coordination should be less important because the emission of TTV derivatives is only slightly affected by peripheral N-substituent groups.[34] Moreover, the fluorescence properties can also be modulated by photoirradiation. The fluorescence intensities of **1**–**3** were gradually reduced upon irradiation using a 300 W xenon lamp and the quenching efficiency reaches 95.84% (464 nm for compound **1**), 82.82% (463 nm for compound **2**) and 90.14% (466 nm for compound **3**) of the original values in their individual photochromism saturation of 35, 105 and 30 minutes, respectively, which further supports that complexes **1**–**3** cause an electron-transfer process upon irradiation. Table 2 summarized the quenching efficiency of fluorescence intensities for several similar systems of extended viologens and naphthalenediimide. As we can see, the significant value of 95.84% of **1** is the highest quenching efficiency as far as we know.

Similarly, according to the Lambert–Beer law, $\ln[(F_0 - F)/(F_t - F)] = kt$ and the first-order kinetics, the photo-controlled fluorescence spectra at 464 nm for **1** (463 nm for **2** and 466 nm for **3**) can be linearly fitted. The rate constants (k) are 4.48×10^{-3} s^{-1} (R^2 = 0.9969) for **1**, 6.72×10^{-4} s^{-1} (R^2 = 0.9870) for **2** and 9.34×10^{-4} s^{-1} (R^2 = 0.9838) for **3**, respectively (Fig. 7).

Table 2 The quenching efficiency of fluorescence intensities for some compounds of extended viologens and naphthalenediimide

Compound	Quenching efficiency	Reference
m-TTzPA	95.84%	This work
$\{[Cd(m\text{-}TTzPA)Br_2]\cdot H_2O\}_n$	82.82%	This work
$\{[Zn(m\text{-}TTzPA)Br_2]\cdot H_2O\}_n$	90.14%	This work
$[Zn_2(bpdc)_2(m\text{-}DPNDI)_2]\cdot H_2O$[a]	21%	35
$[Cd(bpdc)(m\text{-}DPNDI)]\cdot H_2O$[a]	30%	35
$[Zn(3\text{-}NDI)_{0.5}(NDC)(DMF)]_n$[b]	73.7%	36
$\{[Zn_{1.5}(3\text{-}NDI)_{0.5}(BDC)_{1.5}]\cdot 2.5DMF\}_n$[b]	41.1%	36
$[ZnL]\cdot 2H_2O$[c]	90%	37
$[Cd_2(TTVTC)Cl_2(H_2O)_3]\cdot 2H_2O$[d]	92%	21
$[Eu_2(tcbpta)(ndc)(H_2O)_7Cl]Cl_3\cdot 4H_2O\cdot EtOH$[e]	91%	38
$(H_2TTVP)_{0.5}(H_2BTEC)_{0.5}\cdot H_2O\cdot DMF$[f]	*ca.* 15%	39
$\{[Cd(TTVP)_{0.5}(HBTC)(H_2O)_2]\cdot 2H_2O\}_n$[g]	*ca.* 24%	40

[a] H_2bpdc = 4,4′-diphenic acid, m-DPNDI = *N*,*N*′-bis(3-pyridyl)-1,4,5,8-naphthalenetetracarboxydiimide. [b] 3-NDI = *N*,*N*′-bis(3-pyridine methyl)-1,4,5,8-naphthalenediimide, H_2NDC = 1,4-naphthalenedicarboxylic acid, H_2BDC = terephthalic acid, and DMF = *N*,*N*′-dimethylformamide. [c] L^{2-} = phenylenebis(1-[[3,5-dicarboxylatophenyl]methyl]pyrid-4-yl). [d] TTVTC = 2,5-bis(pyridinium-4-yl)thiazolo[5,4-*d*]thiazole tetracarboxylate. [e] tcbpta = 2,4,6-tris(1-(4-carboxylatobenzyl)pyridinium-4-yl)-1,3,5-triazine, ndc = 2,6-naphthalenedicarboxylate. [f] TTVP = 2,5-bis(pyridinium-4-yl) thiazolo[5,4-*d*]thiazole propionate, H_4BTEC = 1,2,4,5-benzenetricarboxylic acid. [g] TTVP = 2,5-bis(pyridinium-4-yl)thiazolo[5,4-*d*]thiazole propionate, H_3BTC = 1,3,5-benzenetricarboxylic acid.

In general, compounds **1**–**3** cause an electron-transfer process upon irradiation, which is competitive with luminescence emission. Moreover, rate constants (*k*) of photo-controlled fluorescence spectra and photochromic UV-vis spectra are very close for compounds **1**–**3**. Therefore, the photochromic behavior and fluorescence quenching are synchronous and concomitant. The efficiency of fluorescence quenching can be achieved by constructing the photochromic unit and accelerating the photochromic speed.

Conclusions

Two new coordination polymers, $\{[Cd(m\text{-}TTzPA)Br_2]\cdot H_2O\}_n$ (**2**) and $\{[Zn(m\text{-}TTzPA)Br_2]\cdot H_2O\}_n$ (**3**), were synthesized based on *N*,*N*′-2,5-bis(3-pyridinium)thiazolo[5,4-*d*]thiazole dipropionic acid hydrogen sulfite, $(m\text{-}H_2TTzPA)(HSO_3)_2$ (**1**). The combination of N-donor ligands and carboxylic ligands constitutes a complete electron donor and acceptor pair. A photoinduced electron transfer process can occur in compounds **1**–**3** upon irradiation and was confirmed by single-crystal X-ray diffraction, UV-vis spectra and EPR characterizations. Upon irradiation by a xenon lamp (300 W), all the compounds have obvious fluorescence quenching behaviors and the quenching efficiency reaches 95.84% for compound **1**. The photomodulable luminescence properties have potential applications in molecular switches, information storage and anti-counterfeiting.

Data availability

The data that support the findings of this study are available from the corresponding author upon reasonable request.

Conflicts of interest

There are no conflicts to declare.

Acknowledgements

This work was supported by the National Natural Science Foundation of China (No. 22371138, 21771111 and 21371104).

References

1 M. Irie, *Chem. Rev.*, 2000, **100**, 1685–1716.
2 H. Tian and S.-J. Yang, *Chem. Soc. Rev.*, 2004, **33**, 85–97.
3 M.- S. Wang, G. Xu, Z.- J. Zhang and G.- C. Guo, *Chem. Commun.*, 2010, **46**, 361–376.
4 L.-Z. Cai, Q.-S. Chen, C.-J. Zhang, P.-X. Li, M.-S. Wang and G.-C. Guo, *J. Am. Chem. Soc.*, 2015, **137**, 10882–10885.
5 B. Xia, Y. Zhou, Q.-L. Wang, X.-F. Xu, Y.-Z. Tong, X.-H. Bu and J.-R. Li, *Dalton Trans.*, 2018, **47**, 15888–15896.
6 B. Xia, Q. Gao, Z.-P. Hu, Q.-L. Wang, X.-W. Cao, W. Li, Y. Song and X.-H. Bu, *Research*, 2021, 5490482.
7 B. Garai, A. Mallick and R. Banerjee, *Chem. Sci.*, 2016, **7**, 2195–2200.
8 J. Kärnbratt, M. Hammarson, S.-M. Li, H. L. Anderson, B. Albinsson and J. Andréasson, *Am. Ethnol.*, 2010, **122**, 1898–1901.
9 J.-J. Zhang, Q. Zou and H. Tian, *Adv. Mater.*, 2013, **25**, 378–399.
10 W. Wan, M.-Q. Zhu, Z. Tian and A. D. Q. Li, *J. Am. Chem. Soc.*, 2015, **137**, 4312–4315.
11 W.-Q. Liao, Y.-L. Zeng, Y.-Y. Tang, Y.-Q. Xu, X.-Y. Huang, H. Yu, H.-P. Lv, X.-G. Chen and R.-G. Xiong, *Adv. Mater.*, 2023, **35**, 2305471.
12 S. Castellanos, F. Kapteijn and J. Gascon, *CrystEngComm*, 2016, **18**, 4006–4012.
13 R. Lyndon, K. Konstas, B. P. Ladewig, P. D. Southon, P. C. J. Kepert and M. R. Hill, *Angew. Chem., Int. Ed.*, 2013, **52**, 3695–3698.
14 D. A. Sherman, R. Murase, S. G. Duyker, Q. Gu, W. Lewis, T. Lu, Y. Liu and D. M. D'Alessandro, *Nat. Commun.*, 2020, **11**, 2808.

15 Y.-J. Ma, J.-X. Hu, S.-D. Han, J. Pan, J.-H. Li and G.-M. Wang, *J. Am. Chem. Soc.*, 2020, **142**, 2682–2689.
16 D.-X. Feng, Y. Mu, J. Li, S.-D. Han, J.-H. Li, H.-L. Sun, M. Pan, J.-X. Hu and G.-M. Wang, *Adv. Funct. Mater.*, 2023, **33**, 2305796.
17 J.- K. Sun, X.-D. Yang, G.- Y. Yang and J. Zhang, *Coord. Chem. Rev.*, 2019, **378**, 533–560.
18 Z.-W. Chen, G. Lu, P.-X. Li, R.-G. Lin, L.-Z. Cai, M.-S. Wang and G.-C. Guo, *Cryst. Growth Des.*, 2014, **14**, 2527–2531.
19 W. W. Porter III, T. P. Vaid and A. L. Rheingold, *J. Am. Chem. Soc.*, 2005, **127**, 16559–16566.
20 A. N. Woodward, J. M. Kolesar, S. R. Hall, N.-N. Saleh, D. S. Jones and M. G. Walter, *J. Am. Chem. Soc.*, 2017, **139**, 8467–8473.
21 P. Li, M.-Y. Guo, X.-M. Yin, L.-L. Gao, S.-L. Yang, R. Bu, T. Gong and E.-Q. Gao, *Inorg. Chem.*, 2019, **58**, 14167–14174.
22 K.-P. Chen, W.-J. Xu, Y. Ma and Q.-L. Wang, *Cryst. Growth Des.*, 2022, **22**, 1024–1031.
23 J. Luo, B. Hu, C. Debruler and T. L. Liu, *Angew. Chem., Int. Ed.*, 2018, **57**, 231–235.
24 G. M. Sheldrick, *Acta Crystallogr., Sect. C: Struct. Chem.*, 2015, **71**, 3–8.
25 M. Fugel, D. Jayatilaka, E. Hupf, J. Overgaard, V. R. Hathwar, P. Macchi, M. J. Turner, J. A. K. Howard, O. V. Dolomanov, H. Puschmann, B. B. Iversen, H.-B. Bürgi and S. Grabowsky, *IUCrJ*, 2018, **5**, 32–44.
26 J. Tarábek, J. Wen, P. I. Dron, L. Pospíšil and J. Michl, *J. Org. Chem.*, 2018, **83**, 5474–5479.
27 A.-J. Liu, F. Xu, S.-D. Han, J. Pan and G.-M. Wang, *Cryst. Growth Des.*, 2020, **20**, 7350–7355.
28 C.-J. Zhang, Z.-W. Chen, R.-G. Lin, M.-J. Zhang, P.-X. Li, M.-S. Wang and G.-C. Guo, *Inorg. Chem.*, 2014, **53**, 847–851.
29 Y.-J. Ma, J.-X. Hu, S.-D. Han, J. Pan, J.-H. Li and G.-M. Wang, *Chem. Commun.*, 2019, **55**, 5631–5634.
30 J. Zhang, Y. Zeng, H.-C. Lu, X.-H. Chen, X.-Z. Yuan and Z.-Y. Fu, *Cryst. Growth Des.*, 2020, **20**, 2617–2622.
31 C. Fu, H.-Y. Wang, G.-S. Zhang, L. Li, Y.-N. Sun, J.-W. Fu and H. Zhang, *CrystEngComm*, 2018, **20**, 4849–4856.
32 T. Liu, Y. Chen, Z.-L. Sun, J. Liu and J.-J. Liu, *J. Solid State Chem.*, 2019, **277**, 216–220.
33 J.-J. Liu, Y.-F. Guan, Y. Chen, M.-J. Lin, C.-C. Huang and W.-X. Dai, *Dalton Trans.*, 2015, **44**, 17312–17317.
34 A. N. Woodward, J. M. Kolesar, S. R. Hall, N.-A. Saleh, D. S. Jones and M. G. Walter, *J. Am. Chem. Soc.*, 2017, **139**, 8467–8473.
35 L.-T. Zhang, B. Xia, X. Zhang, S. Lu, X.-X. Zhou, Q.-W. Li and Q.-L. Wang, *CrystEngComm*, 2021, **23**, 140–145.
36 Y.-J. Wang, S.-Y. Wang, Y. Zhang, B. Xia, Q.-W. Li, Q.-L. Wang and Yue Ma, *CrystEngComm*, 2020, **22**, 5162–5169.
37 P. Li, L.-J. Zhou, N.-N. Yang, Q. Sui, T. Gong and E.-Q. Gao, *Cryst. Growth Des.*, 2018, **18**, 7191–7198.
38 G. Li, S.-L. Yang, W.-S. Liu, M.-Y. Guo, X.-Y. Liu, R. Bu and E.-Q. Gao, *Inorg. Chem. Front.*, 2021, **8**, 4828–4837.
39 F. Yang, J. Chen, J. Wang and J. Liu, *CrystEngComm*, 2023, **25**, 5461–5469.
40 F. Yang, J. Chen, Y. Fu, J. Wang and J. Liu, *Dyes Pigm.*, 2024, **222**, 111877.